

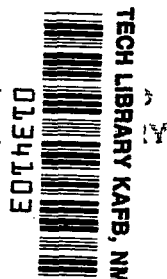
NASA TECHNICAL NOTE



NASA TN D-8371 *cl*

NASA TN D-8371

LOAN COPY: RE
AFWL TECHNICAL
KIRTLAND AFB



**THE EFFECT OF DIGITAL COMPUTING
ON THE PERFORMANCE OF A CLOSED-LOOP
CONTROL-LOADING SYSTEM**

Russell V. Parrish and Billy R. Ashworth

Langley Research Center

Hampton, Va. 23665



NATIONAL AERONAUTICS AND SPACE ADMINISTRATION • WASHINGTON, D. C. • DECEMBER 1976



0134103

1. Report No. NASA TN D-8371		2. Government Accession No.		5. Report Date December 1976	
4. Title and Subtitle THE EFFECT OF DIGITAL COMPUTING ON THE PERFORMANCE OF A CLOSED-LOOP CONTROL-LOADING SYSTEM				6. Performing Organization Code	
7. Author(s) Russell V. Parrish and Billy R. Ashworth				8. Performing Organization Report No. L-11156	
9. Performing Organization Name and Address NASA Langley Research Center Hampton, VA 23665				10. Work Unit No. 505-09-41-01	
12. Sponsoring Agency Name and Address National Aeronautics and Space Administration Washington, DC 20546				11. Contract or Grant No.	
				13. Type of Report and Period Covered Technical Note	
15. Supplementary Notes				14. Sponsoring Agency Code	
16. Abstract <p>A sampled data model of a control loader system for flight simulation has been developed and successfully validated. The model accounts for the effects of the central digital simulation computer on the response of the analog control loader system and includes the spring-gradient, bob-weight, and actuator-lag effects of the aircraft. The revelation of a frequency error introduced by the implementation of force feedback through the digital computer that could adversely affect pilot performance in simulated flight has led to a proposed new implementation which will minimize the impact of the frequency problem.</p>					
17. Key Words (Suggested by Author(s)) Sampled data feedback Control loading systems Aircraft controls			18. Distribution Statement Unclassified - Unlimited Subject Category 05		
19. Security Classif. (of this report) Unclassified	20. Security Classif. (of this page) Unclassified	21. No. of Pages 30	22. Price* \$3.75		

THE EFFECT OF DIGITAL COMPUTING ON THE PERFORMANCE
OF A CLOSED-LOOP CONTROL-LOADING SYSTEM

Russell V. Parrish and Billy R. Ashworth
Langley Research Center

SUMMARY

A sampled data model of a control loader system for flight simulation has been developed and successfully validated. The model accounts for the effects of the central digital simulation computer on the response of the analog control loader system and includes the spring-gradient, bob-weight, and actuator-lag effects of the aircraft. The revelation of a frequency error introduced by the implementation of force feedback through the digital computer that could adversely affect pilot performance in simulated flight has led to a proposed new implementation which will minimize the impact of the frequency problem.

INTRODUCTION

For several years, the Langley differential maneuvering simulator (DMS) has been used to provide a realistic means of simulating two aircraft operating in a differential mode. The system consists of two identical fixed-base cockpits and projection systems, each housed in a 12.2-m-diameter (40-ft) spherical projection screen. Each projection system consists of a sky-Earth projector and a system for target-image generation and projection. The cockpits are provided with typical instrumentation, g-suits, programmable buffet mechanisms, and programmable control forces. The system, as shown in figure 1, was designed to accommodate simulation of a wide range of aircraft performance. (See ref. 1.)

The programmable control forces are a small part of the overall system, but play a large role in providing the pilot with kinesthetic cues. Each cockpit is equipped with programmable, hydraulic, control-loading servos in all three axes. The system can be programmed for preset nonlinear spring gradients, damping, friction, breakout, dead band, and electrical stops. Each axis also has inputs for computer-generated forces which are a function of the aircraft dynamic situation. These forces, due to aerodynamic effects, bob weights, and so forth, are programmed in the central digital computer, along with the two aircraft models, the relative geometry, and the projection drive equations.

During continued use of the system, it became standard practice to adjust the hardware damping in the pitch axis to well above the value specified for critical damping, whenever computer-generated spring gradients or bob-weight dynamics were employed. This procedure was necessary in order to maintain a critically damped system and, in some cases, to avoid instability. In order to understand the reasons for this increase in required damping, a linear analysis using sampled data theory was carried out.

The sampled data model derived to simulate the closed-loop control-loading system included the representation of a linear control-loader servo with digital feedback of spring gradient forces and, if desired, bob-weight forces. A representative actuator lag for the elevator could also be included. The recursive equation solution of this model was validated with a hybrid simulation of a linear control-loader servo with digital gradient force feedback only and also with the DMS control force system as used in an actual flight simulation, both without and with bob-weight effects.

With the successful validation of the recursive equation solution, a tool was available for the selection of the hardware damping of the DMS to insure a properly damped system for a range of spring gradients, bob weights, and actuator lags. More significantly, however, use of the model revealed a reduction in the natural frequency of the continuous system being simulated with the DMS control force system. The revelation of this frequency error, introduced by the implementation of force feedback through the digital computer, which could adversely affect pilot performance in simulated flight, has led to a proposed new implementation which will minimize the impact of the frequency problem.

SYMBOLS

The measurements and calculations were made in U.S. Customary Units. Values are given in both the International System of Units (SI) and in U.S. Customary Units.

A,B,H	matrices of sampled data model
a_1	parameter of sampled data model, m/N-sec (ft/lb-sec)
a_2	parameter of sampled data model, m/N (ft/lb)
a_3, a_4	parameters of sampled data model, dimensionless
a_5	parameter of sampled data model, rad/m (rad/ft)
b	DMS hardware damping setting, N-sec/m (lb-sec/ft)
b_1	software damping setting, N-sec/m (lb-sec/ft)
$b_{0.7}$	damping setting for $\xi = 0.7$, sampled data model, N-sec/m (lb-sec/ft)
$b_{c,0.7}$	damping setting for $\xi = 0.7$, continuous model, N-sec/m (lb-sec/ft)
C_1	approximately constant portion of normal acceleration, g units
C_2	gradient of normal acceleration with respect to elevator deflecting, g units/rad
C_z	normal-force coefficient

C_{Zq}	$= \frac{\partial C_Z}{\partial \left(\frac{q\bar{c}}{2V} \right)}$ per radian
$C_{Z\alpha}$	slope of normal-force curve, $\partial C_Z / \partial \alpha$, per radian
$C_{Z\delta_e}$	$= \frac{\partial C_Z}{\partial \delta_e}$ per radian
\bar{c}	mean aerodynamic chord, m (ft)
\bar{c}^T	transpose of \bar{c}
$\vec{d}, \vec{c}, \vec{F}_s, \vec{e}, \vec{x}, \vec{y}^*, \vec{r}^*$	vectors of sampled data model
F_p	kinesthetic feedback force, N (lb)
F_s	stick force, N (lb)
$G(\alpha, q)$	portion of normal acceleration, g units
g	acceleration due to gravity, m/sec ² (ft/sec ²)
K	spring gradient, N/m (lb/ft)
K_b	bob-weight gradient, N/g (lb/g)
K_1	effective bob-weight gradient, N/rad (lb/rad)
K_2	elevator gearing gain, rad/m (rad/ft)
m	control loader stick mass, kg (slugs)
m_a	mass of simulated airplane, kg (slugs)
n	index of sample periods
n_Z	normal acceleration, g units
$n_{Z,1}$	portion of normal acceleration, g units
$n_{Z,2}$	portion of normal acceleration directly dependent on elevator position, g units
q	pitching angular velocity, rad/sec
S	variable of integration
S_a	wing area, m ² (ft ²)
s	Laplace operator

T	sample period, sec
t	time
V	true airspeed, m/sec (ft/sec)
x	stick position, m (ft)
x_{analog}	stick position as analog output, m (ft)
x_{digital}	stick position as digital output, m (ft)
z^{-1}	sample data operator denoting a one iteration delay
α	angle of attack, rad
α_t	trim angle of attack, rad
δ_e	elevator deflection angle, rad
$\delta_{e,c}$	hydraulic servo elevator deflection command, rad
$\delta_{e,t}$	elevator deflection angle at trim, rad
δ_s	nonlinear gearing elevator deflection command, rad
θ	pitch angle, rad
ξ	damping factor
ρ	mass density of air, kg/m ³ (slugs/ft ³)
τ	actuator lag, sec
ω_c	natural frequency of continuous system, rad/sec
ω_d	damped natural frequency, rad/sec
ω_n	undamped natural frequency, rad/sec

Abbreviations:

ADC	analog-to-digital converter
DAC	digital-to-analog converter
DMS	differential maneuvering simulator
ZOH	zero-order hold

A dot over a variable indicates the time derivative of the variable. Arrows over symbols indicate vectors.

CONTROL-LOADING SYSTEMS

The aircraft control system converts stick, wheel, and pedal motions into control-surface deflections and provides force feedback cues to the pilot which assist him in evaluating the aircraft's dynamic state. In direct control or power-boasted systems, the reaction forces are a direct percentage of the aerodynamic forces on the control surfaces. In the full-powered systems used in modern high-performance aircraft, no direct aerodynamic feedback is provided to the pilot. Consequently, full-powered control systems employ various "artificial feel" devices for proper force feedback. These "feel" devices typically provide reaction forces to the pilot as functions of such things as aircraft velocity and acceleration (bob weights), stick and control-surface displacement (springs) and rate (dampers), and dynamic pressure on the control surfaces (bellows).

These reaction forces, both direct and artificial, play an important role in the control of an aircraft; consequently, a great deal of effort has gone into accurately loading the controls in flight simulators of the aircraft. Although mechanizations of control loaders vary, they are typically analog-driven hydraulic servos. For any forces dependent on the aircraft's dynamic state, the control loader must interface with the central computer where the aircraft equations of motion are solved. In most modern simulators, most of the computations are done on digital computers.

The effects of discrete computing on the response of the control loader are dependent on the amount of lag introduced by the sampled data properties of the closed-loop system. Figure 2 illustrates the significant control loops for pilot-airframe coupling during pitch control in a high-performance aircraft. Figure 3 illustrates the system used in the DMS to simulate these control loops. In order to carry out the analysis of the closed-loop system, a linear model of the system was developed by using the state variable format.

SAMPLED DATA MODEL

The sampled data model incorporates representations of the control-loader servo, bob-weight dynamics, and a servo actuator of the elevator. The nonlinear control-loader servo system can be approximated with a linear second-order system as follows:

$$\text{Stick force} = F_s = m\ddot{x} + b\dot{x} + Kx + K_b(n_z - 1)$$

In the DMS, the damping parameter b is typically a hardware constant setting, whereas the spring gradient forces Kx and bob-weight effects $K_b n_z$ are supplied by the central digital computer. Modeling of a linear gradient to include the sampled data effects presents few problems, although the modeling of bob-weight effects requires some approximations. Typically, the normal acceleration is determined in the digital computer by an equation similar to the following:

$$n_z = -\frac{1}{2} \frac{\rho V^2 S_a}{m_a g} \left[(C_Z) \alpha_{t, \delta_e, t} + C_{Z_\alpha} (\alpha - \alpha_t) + C_{Z_q} \frac{q \bar{c}}{2V} + C_{Z_{\delta_e}} (\delta_e - \delta_{e, t}) \right]$$

For the purposes of this analysis, the normal acceleration can be broken into two portions as

$$n_z = G(\alpha, q) - \frac{1}{2} \frac{\rho V^2 S_a}{m_a g} C_{Z_{\delta_e}} \delta_e$$

and the assumption must be made that the major high-frequency variations in n_z during pitch control are due to the $C_{Z_{\delta_e}} \delta_e$ term. Thus, under this assumption, and by assuming slowly varying aerodynamic pressure and mass,

$$n_z \approx C_1 + C_2 \delta_e$$

where C_1 and C_2 are constants. With these assumptions, bob-weight effects now can be included in the sampled data model. Models are also included in flight simulators of the servo actuators of the elevators. A first-order lag model is typical; thus,

$$\frac{\delta_e(s)}{x(s)} = \frac{K_2/\tau}{s + \frac{1}{\tau}}$$

The equations to be placed in state variable format for inclusion in the sampled data model are then

$$F_s = m\ddot{x} + b\dot{x} + Kx + K_b C_1 + K_b C_2 \delta_e - K_b$$

$$\dot{\delta}_e = -\frac{1}{\tau} \delta_e + \frac{K_2}{\tau} x$$

Since the system will begin operation in equilibrium conditions ($\ddot{x} = \dot{x} = \dot{\delta}_e = F_s = 0$), $K_b C_1 - K_b$ acts as a trim condition on the initial conditions of x and δ_e . To simplify the model further, the initial conditions are chosen to be zero, and K_1 is defined to be $K_b C_2$. The effects of these assumptions on the validity of the model with bob weights are discussed in a later section.

Figure 4 presents the sampled data model in block diagram form with the equations in state variable format. The one iteration delay between the inputs and outputs of the central digital computer is included in the model (the z^{-1} term), as are the analog-to-digital (ADC) and digital-to-analog (DAC) converters. The provision for additional damping control within the digital computer was also made.

RECURSIVE EQUATION SOLUTION

The solution of the sampled data model for a synchronized step input in stick force may be obtained from state variable methods by assuming the step input is from a sample hold device. The state transition solution, with zero-order hold (ref. 2), is

$$\vec{x}[(n+1)T] = e^{AT} \vec{x}(nT) + \int_0^T e^{A(T-S)}_B \vec{F}_s(S+nT) dS - \int_0^T e^{A(T-S)}_B \vec{y}^*(S+nT) dS \\ - \int_0^T e^{A(T-S)}_B \vec{r}^*(S+nT) dS$$

The elevator actuator solution, without zero order hold (ref. 2), is

$$\delta_e[(n+1)T] = e^{-T/\tau} \delta_e(nT) + \tau (1 - e^{-T/\tau}) \vec{c}^T \vec{x}(nT)$$

where

$$A = \begin{bmatrix} 0 & 1 \\ 0 & -b/m \end{bmatrix} \quad B = \begin{bmatrix} 0 & 0 \\ 0 & 1/m \end{bmatrix} \quad \vec{F}_s = \begin{bmatrix} 0 \\ 1 \end{bmatrix} \\ H = \begin{bmatrix} 0 & 0 \\ K & b_1 \end{bmatrix} \quad \vec{d} = \begin{bmatrix} 0 \\ K_1 \end{bmatrix} \quad \vec{c}^T = \begin{bmatrix} K_2/\tau & 0 \end{bmatrix}$$

$$e^{AT} = \begin{bmatrix} 1 & (m/b)(1 - e^{-bT/m}) \\ 0 & e^{-bT/m} \end{bmatrix} \quad e^{A(T-S)}_B = e^{AT} \begin{bmatrix} 0 & (1/b)(1 - e^{bS/m}) \\ 0 & (1/m)e^{bS/m} \end{bmatrix}$$

In the model,

$$\vec{y}^* = z^{-1} H \vec{x}$$

and

$$\vec{r}^* = \vec{d} \delta_e$$

Substitution of these equations for \vec{y}^* and \vec{r}^* into the state transition solution yields

$$\vec{x}[(n+1)T] = e^{AT} \vec{x}(nT) + \int_0^T e^{A(T-S)}_B \vec{F}_s(S+nT) dS - \int_0^T e^{A(T-S)}_{BH} \vec{x}[(n-1)T] dS \\ - \int_0^T e^{A(T-S)}_B \vec{d} \delta_e(nT) dS$$

where

$$\int_0^T e^{A(T-S)}_B \vec{F}_s(S+nT) dS = \begin{bmatrix} T/b - (m/b^2)(1 - e^{-bT/m}) \\ (1/b)(1 - e^{-bT/m}) \end{bmatrix}$$

$$\int_0^T e^{A(T-S)}_{BH} \ddot{x}[(n-1)T] dS = \begin{bmatrix} \frac{KT}{b} - \frac{Km}{b^2}(1 - e^{-bT/m}) & \frac{b_1T}{b} - \frac{b_1m}{b^2}(1 - e^{-bT/m}) \\ \frac{K}{b}(1 - e^{-bT/m}) & \frac{b_1}{b}(1 - e^{-bT/m}) \end{bmatrix} \\ \times \ddot{x}[(n-1)T]$$

$$\int_0^T e^{A(T-S)}_B \ddot{\delta}_e(nT) dS = \begin{bmatrix} \frac{K_1T}{b} - \frac{K_1m}{b^2}(1 - e^{-bT/m}) \\ \frac{K_1}{b}(1 - e^{-bT/m}) \end{bmatrix} \delta_e(nT)$$

The solution then becomes

$$x[(n+1)T] = x(nT) + ma_1 \dot{x}(nT) + a_2 \{1 - Kx[(n-1)T] - b_1 \dot{x}[(n-1)T] \\ - K_1 \delta_e(nT)\}$$

$$\dot{x}[(n+1)T] = a_3 \dot{x}(nT) + a_1 \{1 - Kx[(n-1)T] - b_1 \dot{x}[(n-1)T] - K_1 \delta_e(nT)\}$$

$$\delta_e(nT) = a_4 \delta_e[(n-1)T] + a_5 x[(n-1)T]$$

where

$$a_1 = \frac{1}{b}(1 - a_3)$$

$$a_2 = \frac{1}{b}(T - ma_1)$$

$$a_3 = e^{-bT/m}$$

$$a_4 = e^{-T/\tau}$$

$$a_5 = K_2(1 - a_4)$$

VALIDATION

The recursive equation solution was validated in a step-by-step manner, beginning with the model without bob-weight effects and then proceeding to the inclusion of bob-weight effects.

Without Bob Weights

Two different input cases were examined for the model without bob weights. The first case was that of a step input in stick force that was synchronized with the sampling elements. The method of validation utilized an analog computer to provide a continuous, linear, second-order model of the control-loader servo. Force feedback was provided by a digital computer as shown in the hybrid setup of figure 5. In order to synchronize the step input with the sampling elements, the step input was generated on the digital computer.

Table I presents a comparison of the first overshoot results from the hybrid solution with those of the recursive solution for the first case, and also with the overshoots that would be obtained from an all-analog implementation (the continuous model) for various damping settings and sampling periods. It should be mentioned that the overshoot values from the recursive equation solution are expected to be low because of the unlikelihood of the peak overshoot occurring at a sampling instant.

The second input case examined was that of a step input that was asynchronous to the sampling elements; this case is more representative of the actual hardware realization, the pilot input being asynchronous to the digital computer. The hybrid solutions were obtained by implementing the step input on the analog computer. The difference between the two cases is illustrated in figure 6. In the first case, the step input on the digital computer has no effect on the position output of the digital computer until $2T$ seconds later. In the second case, with the step implemented on the analog computer, the delay between the step input and the output of the feedback response from the digital computer varies between T and $2T$ seconds, giving on the average, a $3T/2$ delay.

The recursive equation solution was derived for case I, the step input in stick force being synchronized with the sampling elements of the digital computer. However, the solution can be used to also solve the case II problem simply by initializing the position and velocity terms of the control loader servo model correctly.

Table II presents the similar overshoot results for this second case from the continuous model, the hybrid model, and the recursive model, and also from a DMS application utilizing the nonlinear control-loader hardware and the simulation computer without bob-weight effects. The various time delays between analog step input and digital feedback output occurring with each model are also presented. The delay for the recursive model was set at $3T/2$ (by initial conditions on x and \dot{x}), whereas the delays with the hybrid model and the nonlinear hardware varied between T and $2T$, depending upon the time of application of the input.

Bob-Weight Effects

In the derivation of the recursive equation solution with bob-weight effects, the normal acceleration was broken into two parts

$$n_z = G(\alpha, q) - \frac{1}{2} \frac{\rho V^2 S_a}{m_a g} C_{z\delta_e} \delta_e$$

$$n_{z,1} = G(\alpha, q)$$

$$n_{z,2} = - \frac{1}{2} \frac{\rho V^2 S_a}{m_a g} C_{z\delta_e} \delta_e$$

and the assumptions were made that $n_{z,1}$ acts as a low-frequency trim condition on the control stick and that only $n_{z,2}$ contributes to the dynamics of the control stick. The validity of these assumptions is demonstrated in the data of figure 7, for the case of an analog step input to the stick-force command of the control-loader hardware for a DMS simulation of an F5-E aircraft. In figure 7(a), the total normal acceleration contributes through the bob-weight gradient to the stick force, whereas in figure 7(b), only $n_{z,2}$ contributes to the stick force.

Validation of the recursive equation solution with bob-weight effects was obtained from the F5-E simulation with the $n_{z,1}$ term eliminated from the stick-force equation, as in figure 7(b), in order to allow the measurement of position overshoot. The resulting comparisons are presented in table III for two damping settings and two values of bob weight. Figure 8 presents the recursive equation solutions for one damping setting in time history form.

Actuator Lag Effects

Simulation of bob-weight effects requires the inclusion of actuator lags in the model, if any significant lags are present in the aircraft. However, since the actuator lags are typically introduced as simple first-order lags in the simulation model, no additional validation was thought necessary for the inclusion of this lag in the recursive equation model. Figure 9 demonstrates the effects of actuator lags of various magnitudes on the step response of the control stick utilizing the recursive solution model. This additional lag has very little effect on the first overshoot values and has a great effect on the time necessary to reach the equilibrium state. The effect is similar to the trim effect described previously for the $n_{z,1}$ term of the normal acceleration.

FREQUENCY ERROR

With the successful validation of the recursive equation model, a tool was available for the selection of the hardware damping of the DMS to insure a properly damped system for a range of spring gradients, bob weights, and actuator lags. In order to facilitate the selection process of damping settings for future simulations, figure 10 was constructed in terms of the nondimensional abscissa $\omega_c T / 2\pi$. The undamped natural frequency of the control loop in the continuous domain is $\omega_c = [(K + K_1 K_2) / m]^{1/2}$. The damping parameter value for a 0.7 damped continuous system is $b_{c,0.7}$, and the damping parameter value for the 0.7 damped sampled data system is $b_{0.7}$. By the use of figure 10, the

increase in the hardware damping setting required to maintain a 0.7 damped system with the DMS implementation is readily obtained from knowledge of the continuous system and the sample period.

With the introduction of the undamped natural frequency term in the nondimensional abscissa of figure 10, attention was drawn to the estimates of damped natural frequency that could be obtained from the step responses of the sampled data models for further validation. Again, excellent agreement of these estimates was found between the hybrid model, the recursive equation model, and the nonlinear hardware. However, when the undamped natural frequency was calculated

from the estimates of damped natural frequency $\omega_n = \omega_d / \sqrt{1 - \xi^2}$, the values were found to be conspicuously less than the continuous system values. For example, in the F5-E simulation, a damped natural frequency of $\omega_n = 23.49$ rad/sec was estimated, rather than the continuous system frequency $\omega_c = 40.99$ rad/sec. Figure 11 presents these results as the ratio of the sampled data natural frequency and the continuous natural frequency plotted against the nondimensional abscissa $\omega_c T / 2\pi$. As may be seen from this figure, valid simulation of the continuous system with the DMS implementation is possible only for small values of $\omega_c T$.

The possible impact of this frequency error on pilot performance is illustrated in figure 12 in terms of additional phase lag introduced by the DMS implementation at 1 Hz, the heuristic pilot operating frequency. Since the phase margins of high performance aircraft are on the order of 40° , considerable effect on pilot performance is possible with the DMS implementation.

The effect of the frequency error on magnitude, or the gradient force, is presented in figure 13 as gradient force error at 1 Hz. It should be noted that static forces with the DMS implementation are correct, but dynamically the pilot would be flying a heavier stick, since more force would have to be applied to move the stick the same amount of travel than in the continuous case.

A PROPOSED IMPLEMENTATION

The revelation of the frequency error in the DMS implementation led to a proposed new implementation that would avoid the problems of the old implementation. The solution is the inclusion of two analog multipliers in the feedback loops of the continuous hardware system, as shown in figure 14. In this implementation, the spring gradient K rather than the spring gradient force Kx is supplied to the control loader, and the multiplication of K and x is carried out in the continuous domain rather than within the digital simulation. The bob-

weight force $K_b n z$ is resolved in the digital computer into a gradient $\frac{K_b n z}{x}$

which is then added to the spring gradient before output to the stiffness multiplier. System damping is also provided by the digital computer as

$b = 2\xi \sqrt{\frac{K + \frac{K_b n z}{x}}{m}}$, which is then output to the damping multiplier of the continu-

ous control loader system. Since the multiplications are carried out in the continuous domain (no lags in x and \dot{x}), the lags in the gradients and damping due to the digital computer do not affect the system frequency and damping adversely.

CONCLUDING REMARKS

The revelation of the frequency error introduced by the DMS implementation of the control loader, and the possible effect of this error on pilot performance in simulated flight has led to a proposed new implementation of the control loader hardware. Until modification of the hardware, a means of selection of hardware damping to insure a properly damped system, but with reduced natural frequency, for a range of spring gradients, bob weights, and actuator lags is available. Additionally, valuable insight has been gained into the problems associated with the introduction of a digital computer into the feedback of an analog system. These problems for a second-order system are manifested in a reduction in both damping and frequency in comparison with an all-analog (continuous) solution.

Langley Research Center
National Aeronautics and Space Administration
Hampton, VA 23665
November 26, 1976

REFERENCES

1. Ashworth, B. R.; and Kahlbaum, William M., Jr.: Description and Performance of the Langley Differential Maneuvering Simulator. NASA TN D-7304, 1973.
2. Gupta, Someshwar C.; and Hasdorff, Lawrence: Fundamentals of Automatic Control. John Wiley & Sons, Inc., c.1970.

TABLE I.- DIGITAL STEP INPUT OVERSHOOT RESPONSES

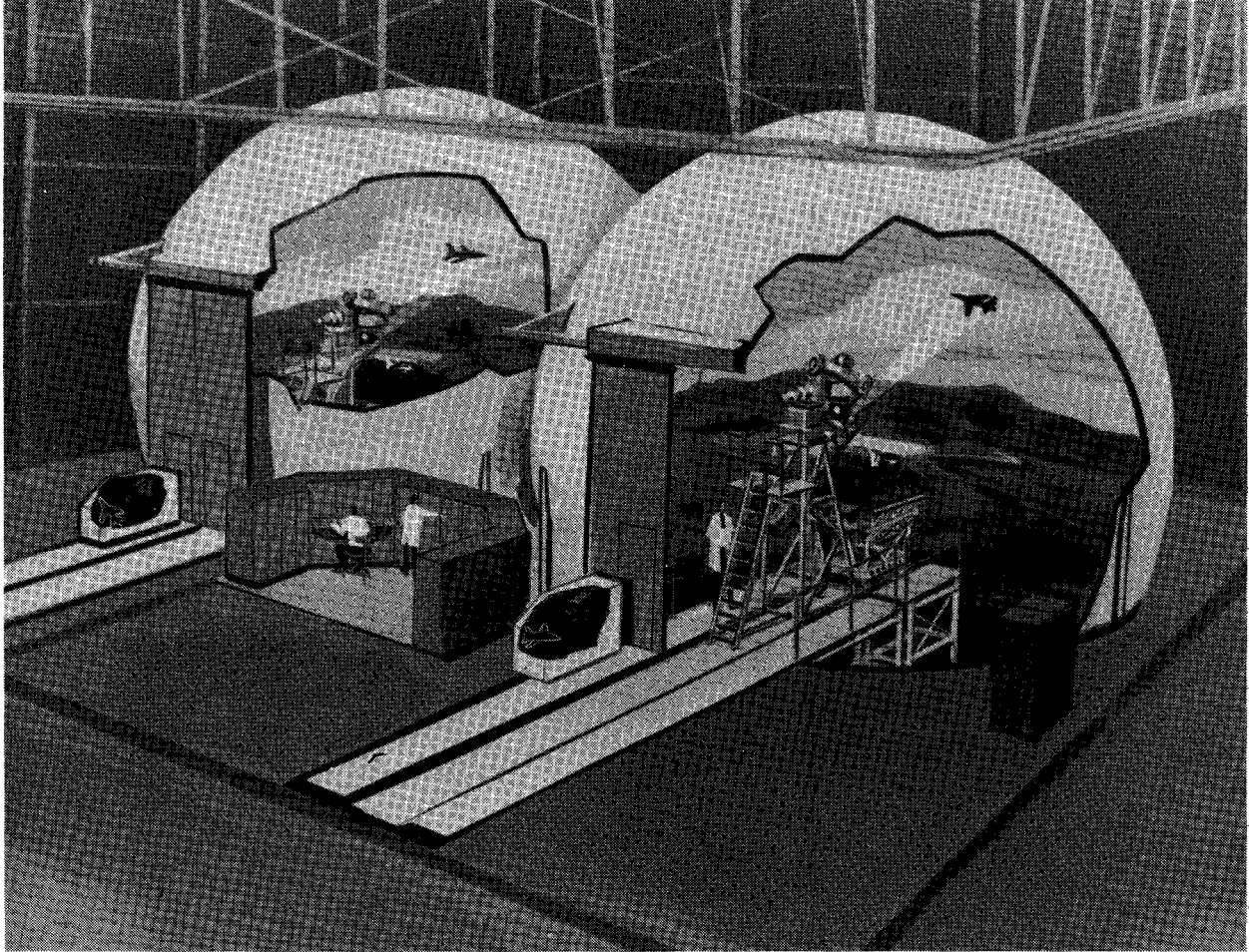
b		Continuous model	Hybrid model	Recursive model
N-sec/m	lb-sec/ft			
T = 1/32 second				
59.835	4.1	1.07	Unstable	Unstable
68.445	4.69	1.02	1.95	1.90
85.520	5.86	1.0	1.64	1.63
102.595	7.03	1.0	1.45	1.44
119.669	8.20	1.0	1.33	1.29
136.890	9.38	1.0	1.22	1.19
153.965	10.55	1.0	1.13	1.12
171.040	11.72	1.0	1.08	1.07
188.114	12.89	1.0	1.04	1.03
205.189	14.06	1.0	1.02	1.01
T = 1/16 second				
102.595	7.03	1.0	Unstable	Unstable
119.669	8.20	1.0	1.99	1.99
136.890	9.38	1.0	1.82	1.81
153.965	10.55	1.0	1.68	1.65
171.040	11.72	1.0	1.55	1.52
188.114	12.89	1.0	1.45	1.41
205.189	14.06	1.0	1.35	1.33

TABLE II.- ANALOG STEP INPUT OVERSHOOT RESPONSES

b		Continuous model	Hybrid model		Recursive model		Nonlinear hardware	
N-sec/m	lb-sec/ft	Overshoot	Delay, msec	Overshoot	Delay, msec	Overshoot	Delay, msec	Overshoot
T = 1/32 second								
59.835	4.1	1.07	55	Unstable	46.875	Unstable	45	1.90
68.445	4.69	1.02	48	1.95	46.875	1.92	60	1.84
85.520	5.86	1.0	45	1.67	46.875	1.61	60	1.66
102.595	7.03	1.0	50	1.48	46.875	1.42	45	1.47
119.669	8.20	1.0	60	1.33	46.875	1.30	60	1.36
136.890	9.38	1.0	38	1.22	46.875	1.19	50	1.25
153.965	10.55	1.0	33	1.14	46.875	1.12	40	1.16
171.040	11.72	1.0	45	1.09	46.875	1.07	42	1.08
188.114	12.89	1.0	53	1.05	46.875	1.03	45	1.03
205.189	14.06	1.0	45	1.03	46.875	1.01	50	1.01
T = 1/16 second								
102.595	7.03	1.0	115	Unstable	93.75	Unstable	93	Unstable
119.669	8.20	1.0	92	1.95	93.75	1.90	95	1.99
136.890	9.38	1.0	67	1.85	93.75	1.69	115	1.86
153.965	10.55	1.0	72	1.68	93.75	1.59	90	1.68
171.040	11.72	1.0	110	1.53	93.75	1.49	100	1.56
188.114	12.89	1.0	120	1.44	93.75	1.41	75	1.45
205.189	14.06	1.0	78	1.36	93.75	1.33	82	1.34

TABLE III.- BOB-WEIGHT OVERSHOOT RESULTS

Model	Damping parameter, b		K _b		Overshoot
	N-sec/m	lb-sec/ft	N/g	lb/g	
Recursive	85.52	5.86	0	0	1.64
Hardware	85.52	5.86	0	0	1.66
Recursive	85.52	5.86	22.24	5	1.67
Hardware	85.52	5.86	22.24	5	1.70
Recursive	85.52	5.86	44.48	10	1.71
Hardware	85.52	5.86	44.48	10	1.76
Recursive	171.04	11.72	0	0	1.07
Hardware	171.04	11.72	0	0	1.08
Recursive	171.04	11.72	22.24	5	1.09
Hardware	171.04	11.72	22.24	5	1.10
Recursive	171.04	11.72	44.48	10	1.11
Hardware	171.04	11.72	44.48	10	1.13



L-76-7513

Figure 1.- Langley differential maneuvering simulator.

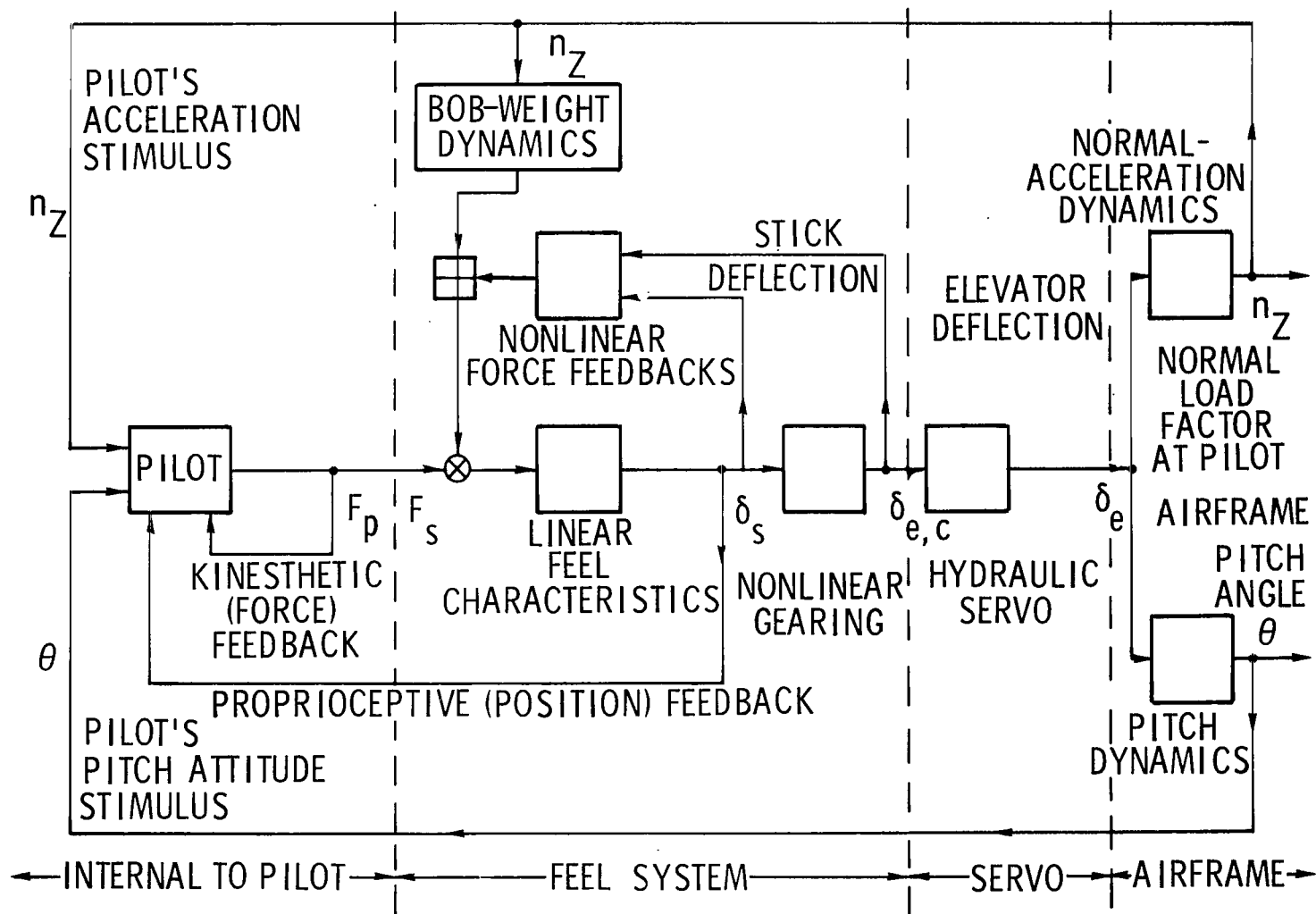


Figure 2.- Significant control loops for pilot-airframe coupling during pitch control.

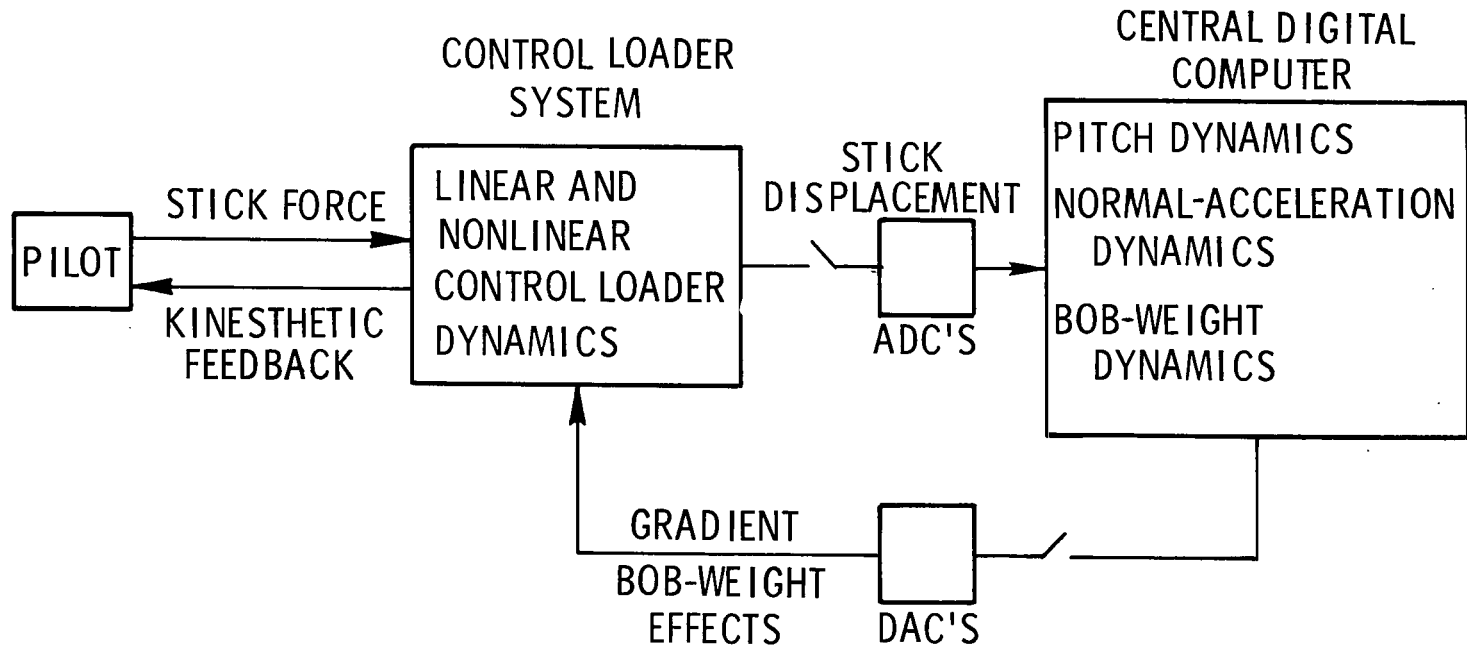
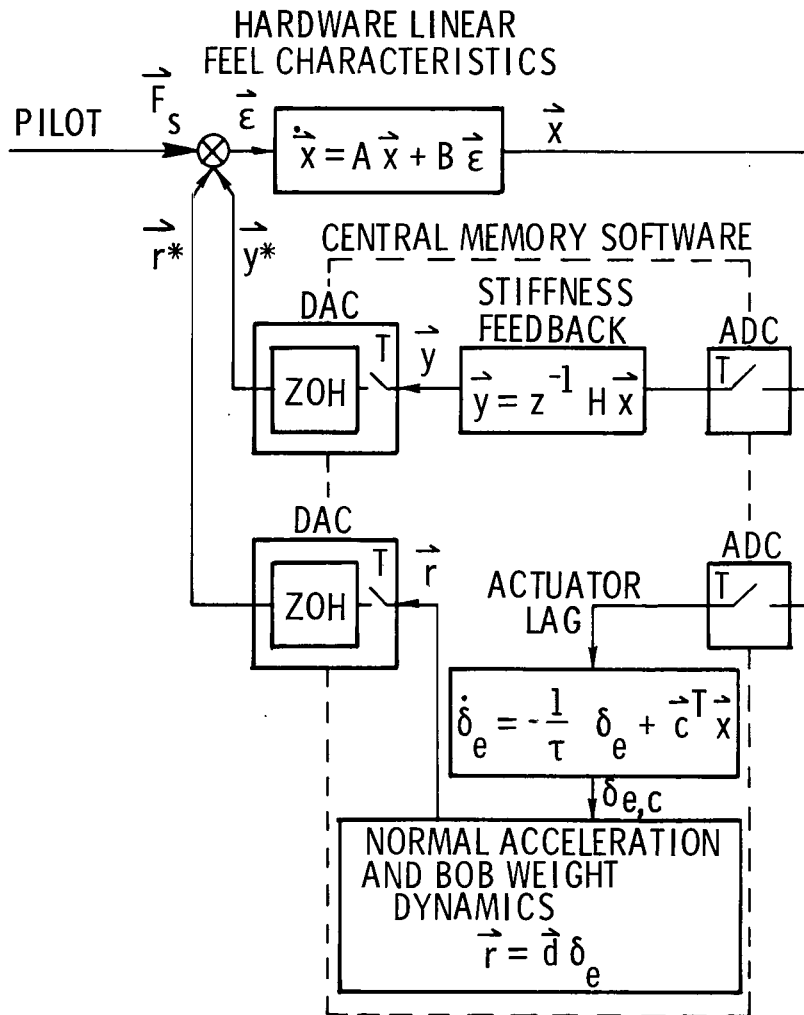


Figure 3.- Differential maneuvering simulator (DMS) pitch control loop.



$$\vec{F}_s = \begin{bmatrix} 0 \\ 1 \end{bmatrix}$$

$$A = \begin{bmatrix} 0 & 1 \\ 0 & -b/m \end{bmatrix}$$

$$B = \begin{bmatrix} 0 & 0 \\ 0 & 1/m \end{bmatrix}$$

$$H = \begin{bmatrix} 0 & 0 \\ K & b_1 \end{bmatrix}$$

$$\vec{d} = \begin{bmatrix} 0 \\ K_1 \end{bmatrix}$$

$$\vec{c}^T = \begin{bmatrix} K_2/\tau & 0 \end{bmatrix}$$

m = MASS

K, K_1 = EFFECTIVE STIFFNESS

b, b_1 = EFFECTIVE DAMPING

τ = ACTUATOR LAG

z^{-1} = ONE COMPUTING ITERATION DELAY

Figure 4.- Sampled data model.

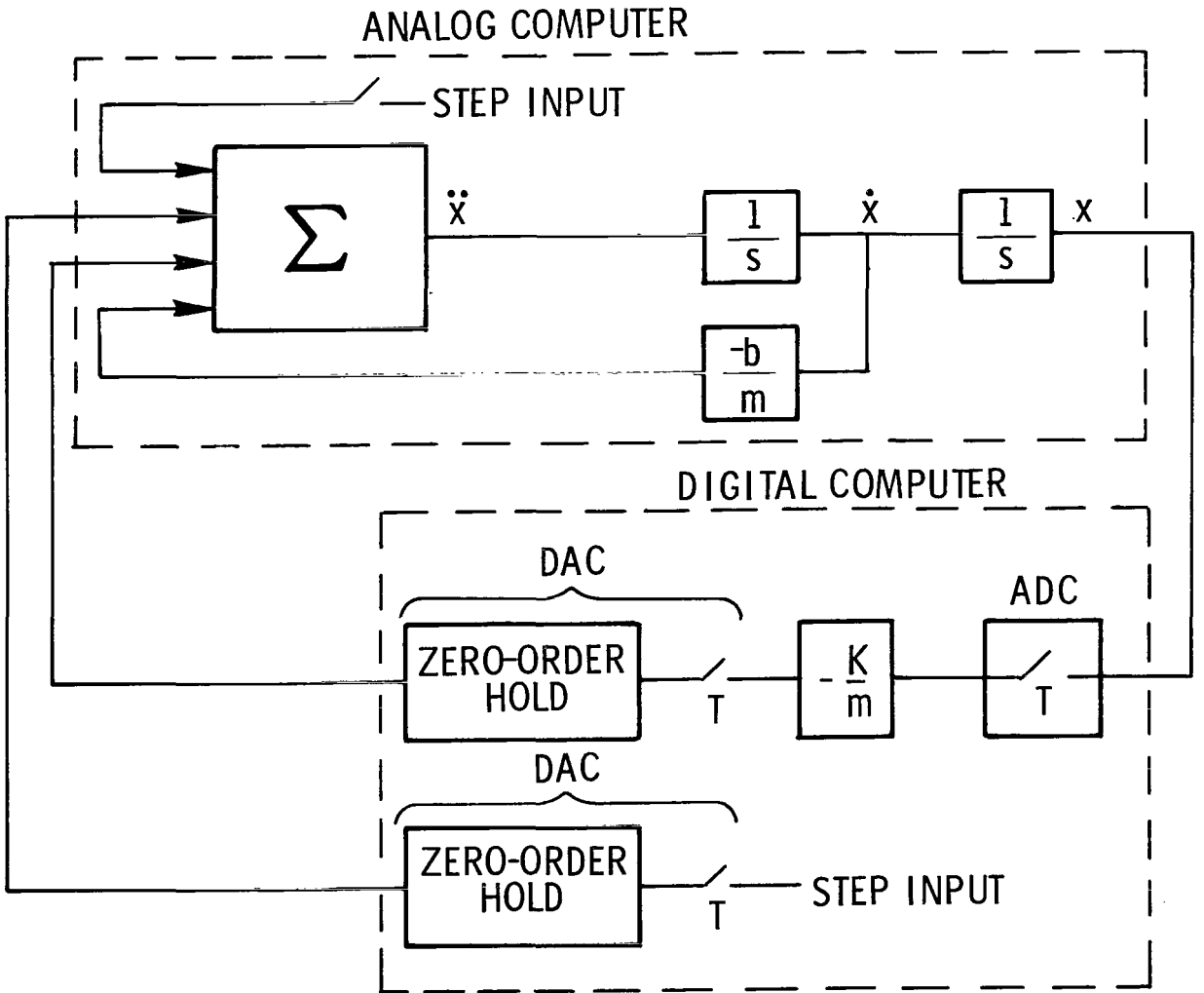


Figure 5.- Hybrid setup of linear pitch control loop.

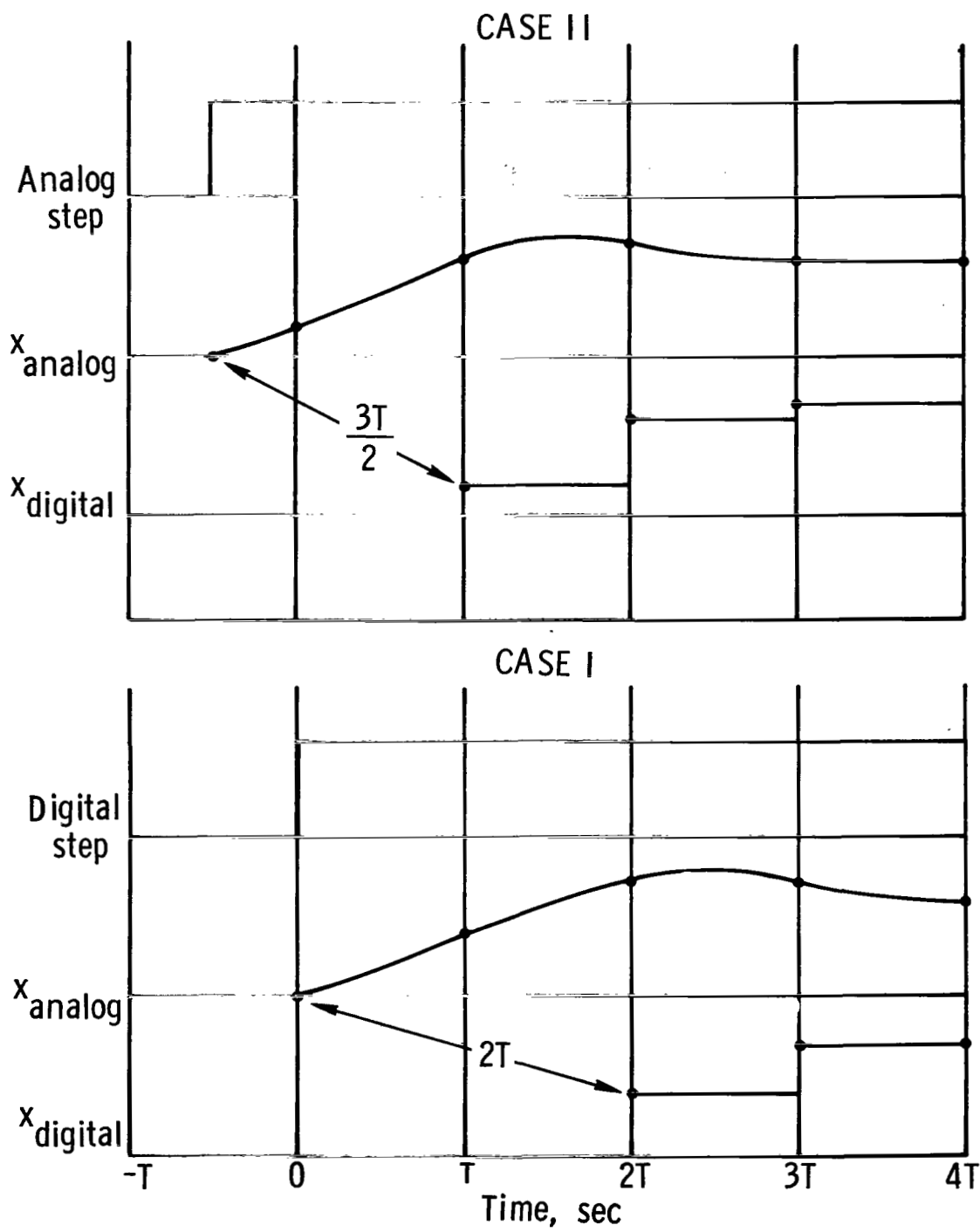
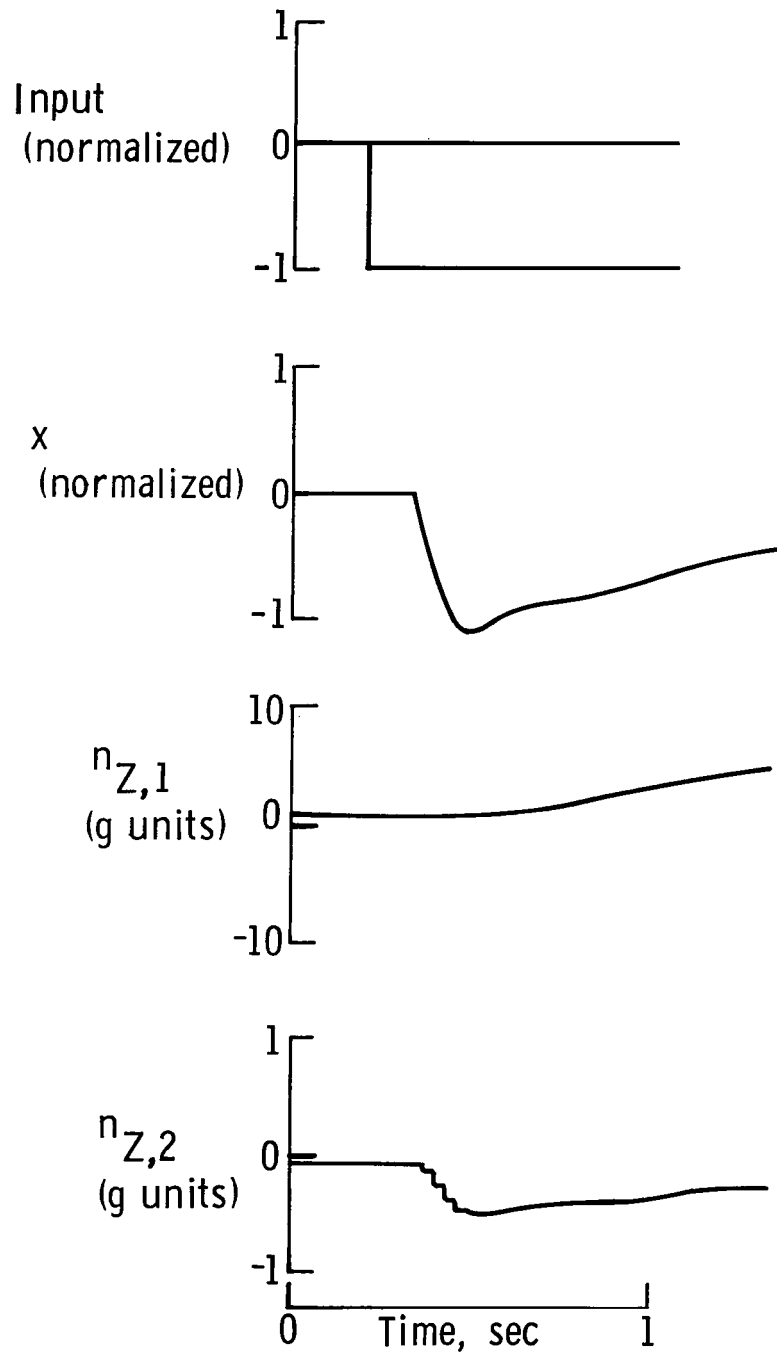
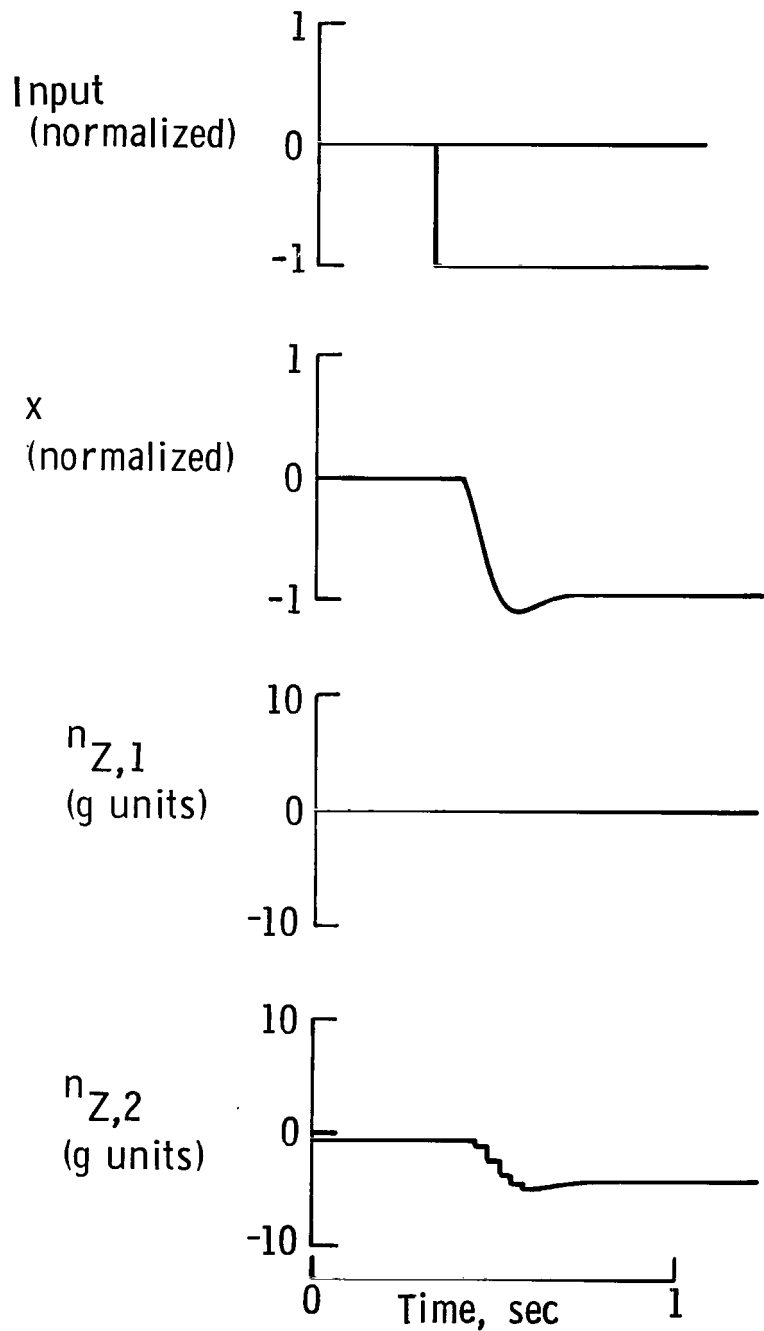


Figure 6.- Timing sequences.



(a) $F_s = m\ddot{x} + bx + Kx + K_b(n_{Z,1} + n_{Z,2} - 1)$.

Figure 7.- Bob-weight effects from F5-E simulation.



(b) $F_s = m\ddot{x} + b\dot{x} + Kx + K_b n_{Z,2}$.

Figure 7.- Concluded.

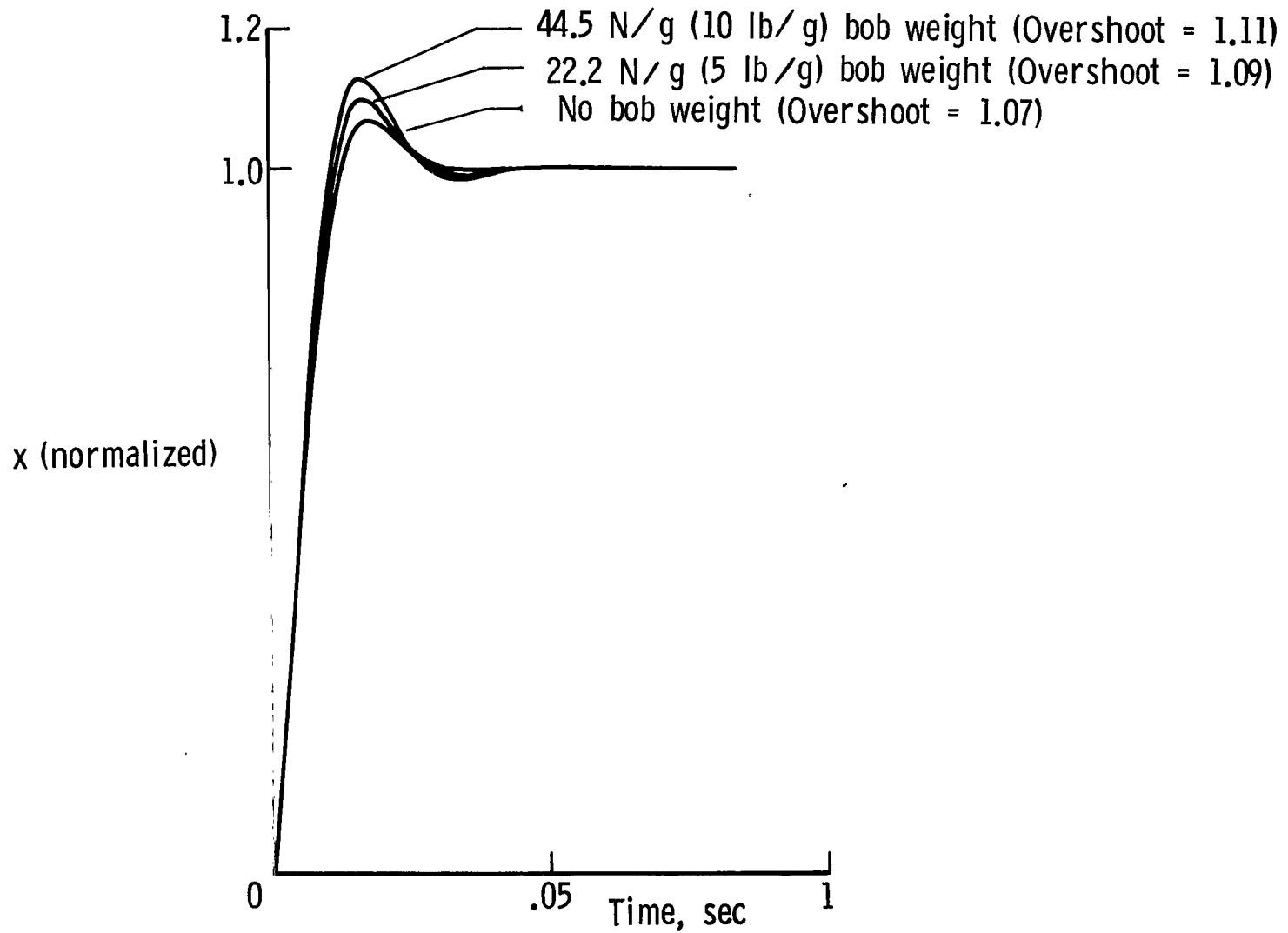


Figure 8.- Bob-weight effects from sampled data model. $b = 171.04$ N-sec/m (11.72 lb-sec/ft); $m = 1.042$ kg (1/14 slugs); $K = 1751.26$ N/m (120 lb/ft); $T = 1/32$ sec; $K_1 = 0$, 24.465 N/rad (5.5 lb/rad), 48.930 N/rad (11 lb/rad); and $K_2 = 0.3048$ rad/m (1 rad/ft).

x (normalized)

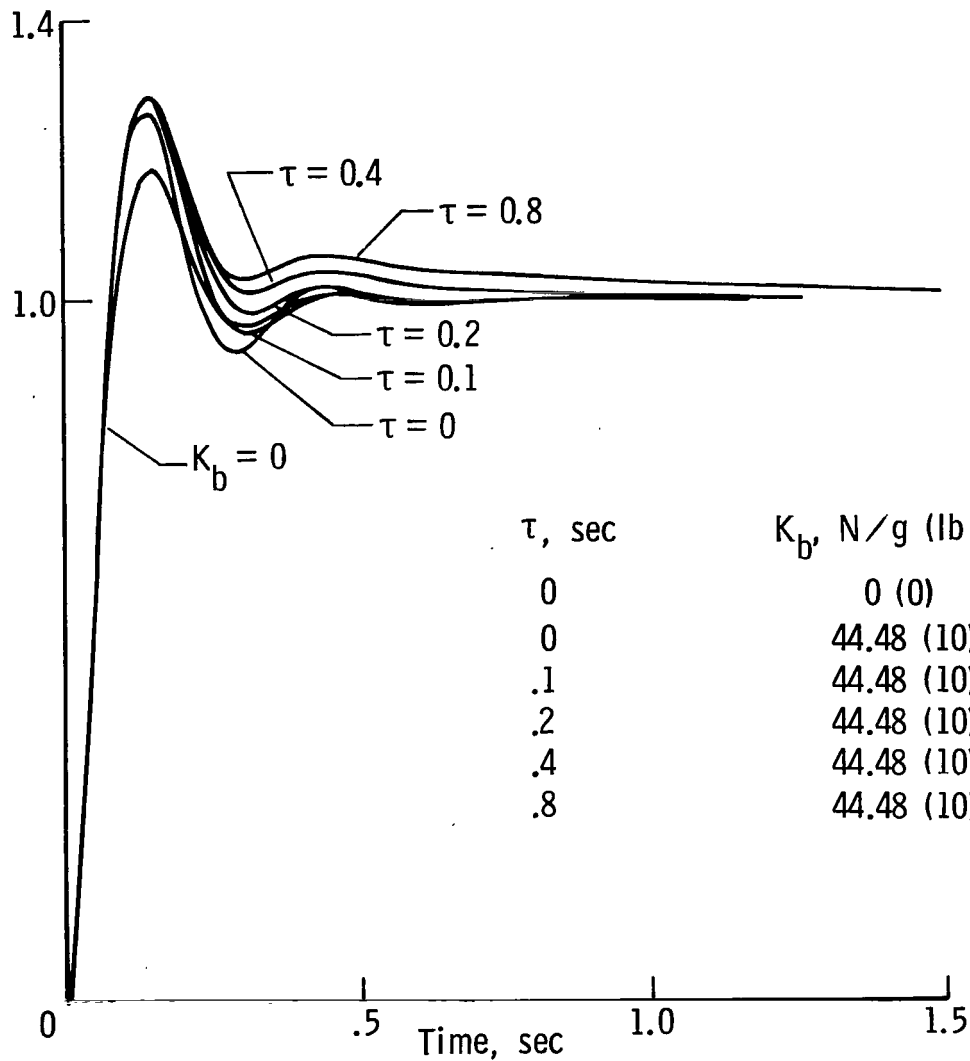


Figure 9.- Actuator lag effects from sampled data model. $b = 136.89$ N-sec/m (9.38 lb-sec/ft); $m = 1.042$ kg (1/14 slugs); $K = 1751.26$ N/m (120 lb/ft); $T = 1/32$ sec; $K_b = 44.48$ N/g (10 lb/g); $K_1 = 48.93$ N/rad (11 lb/rad); and $K_2 = 0.3048$ rad/m (1 rad/ft).

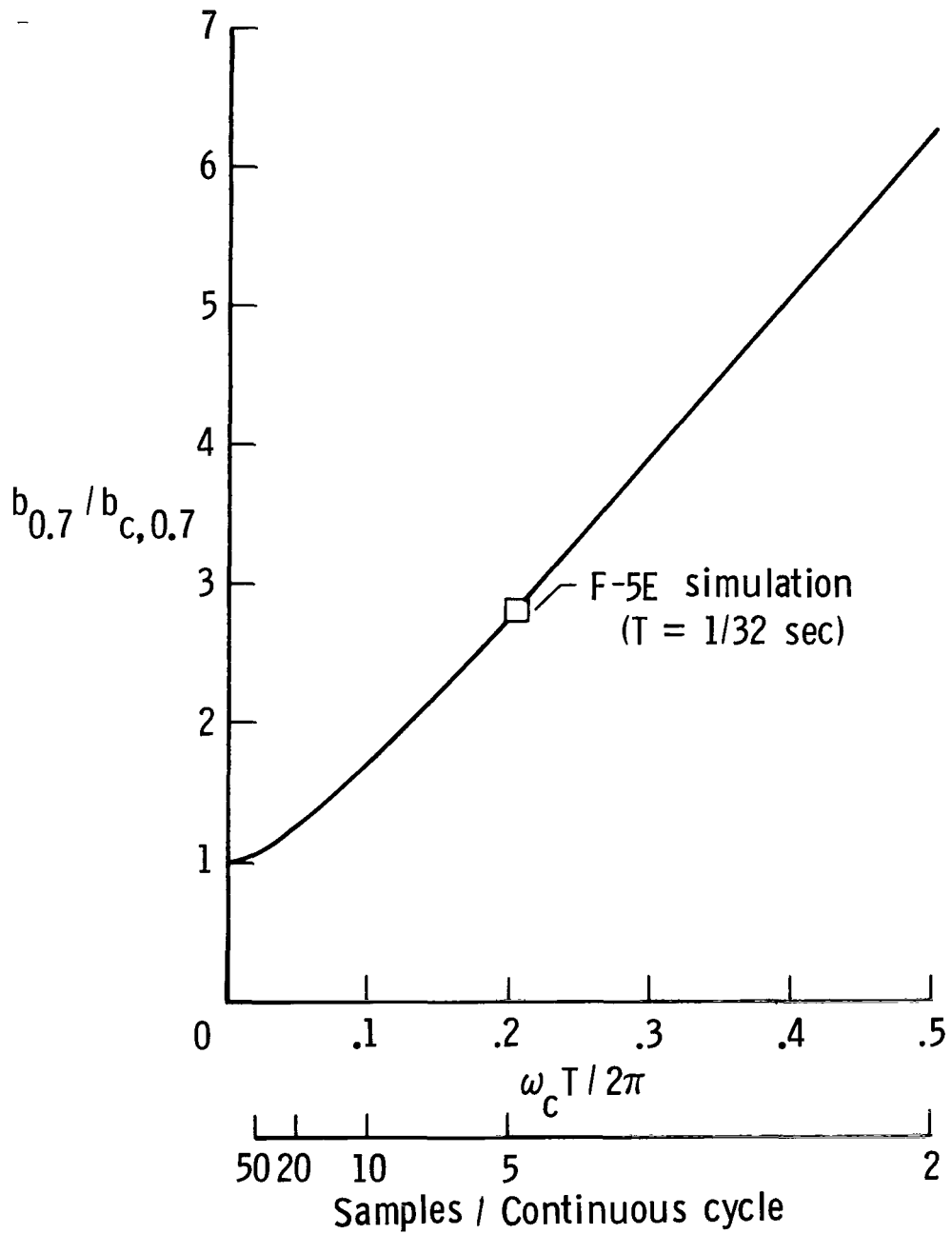


Figure 10.- Ratio of sampled data damping setting to continuous system damping setting for $\xi = 0.7$.

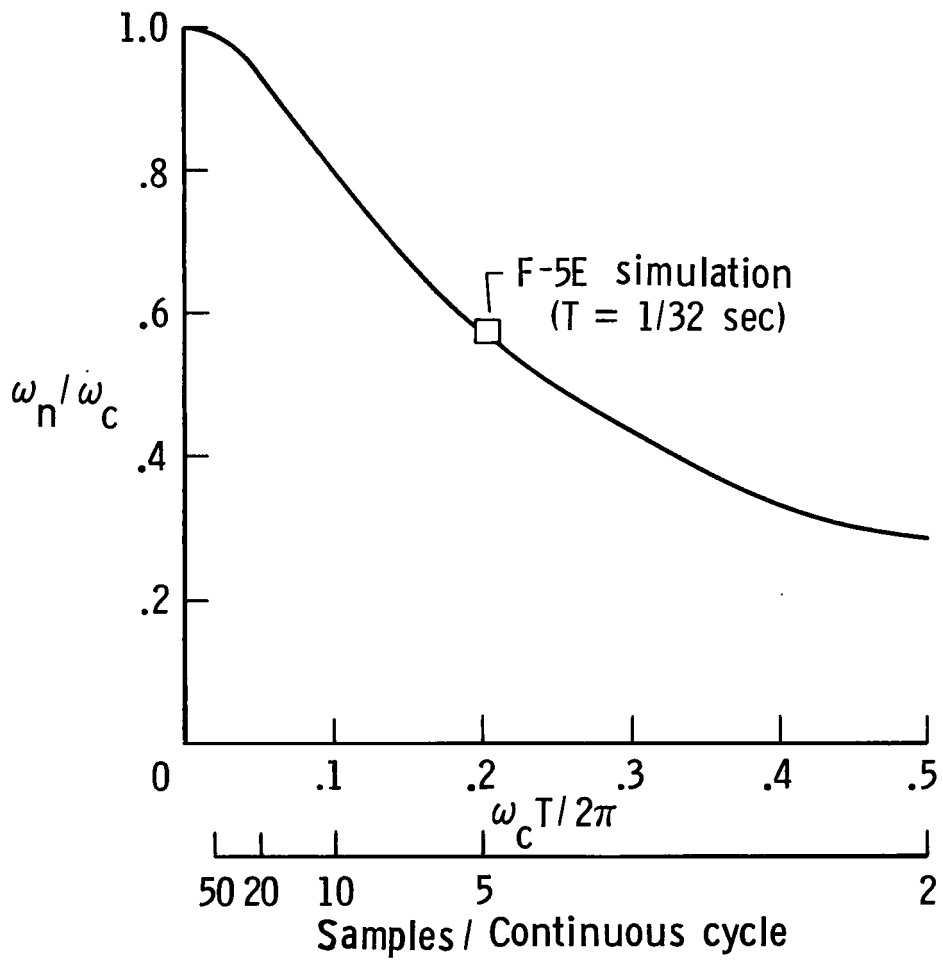


Figure 11.- Ratio of sampled data natural frequency to continuous system natural frequency.

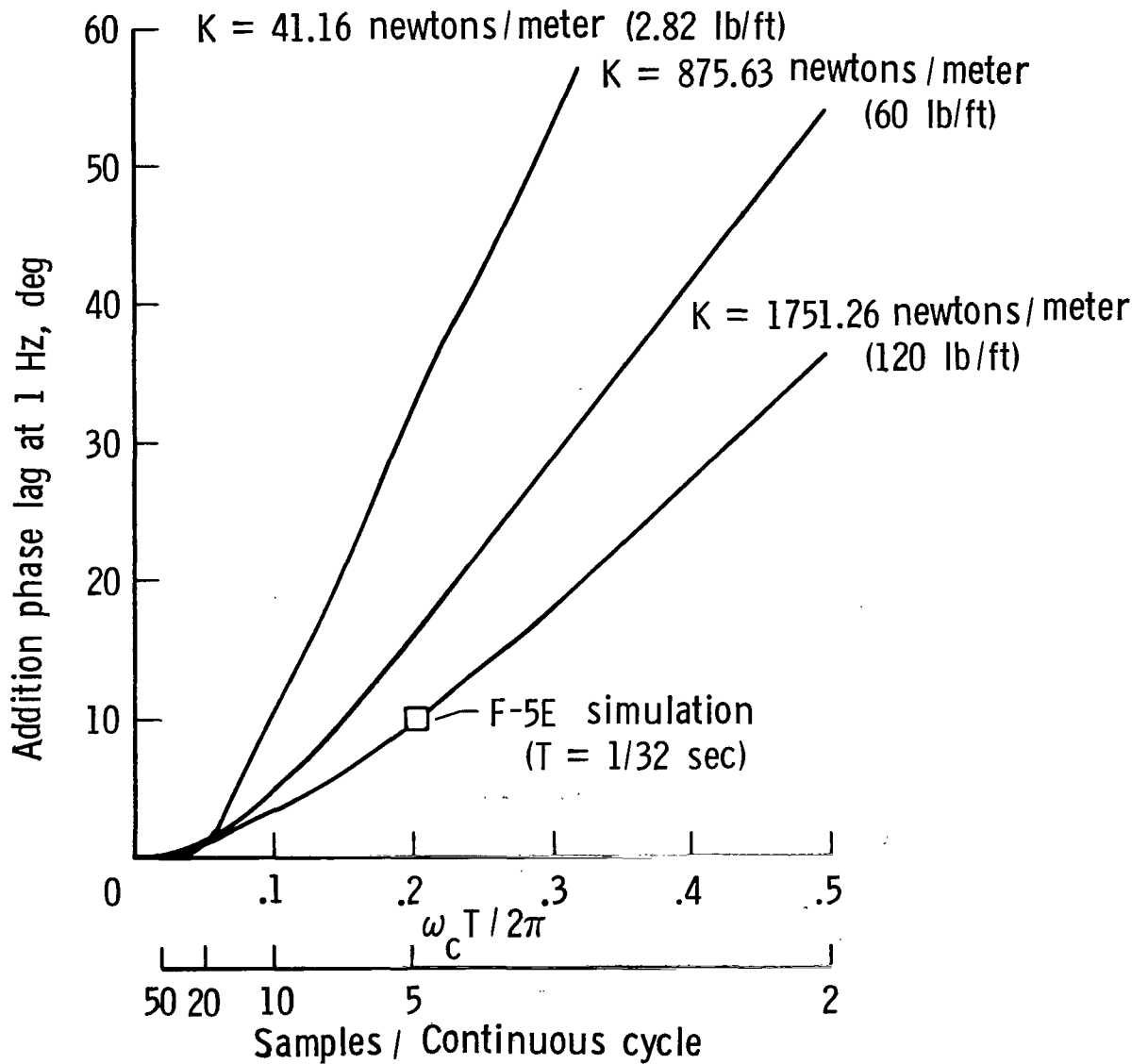


Figure 12.- Additional phase lag at 1 Hz for three spring gradient values ($\xi = 0.7$).

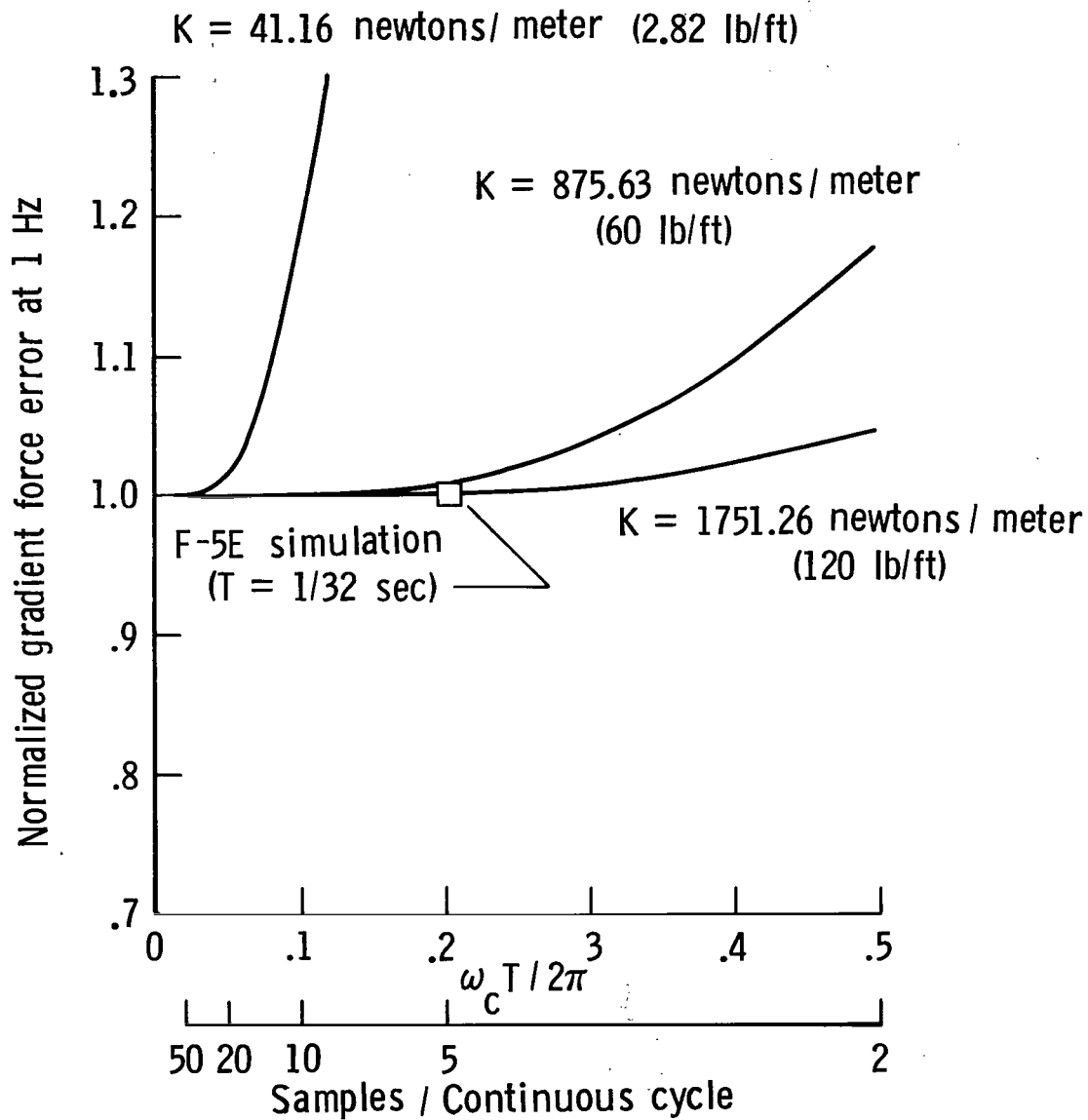


Figure 13.- Dynamic gradient force error at 1 Hz for three spring gradient values ($\xi = 0.7$).

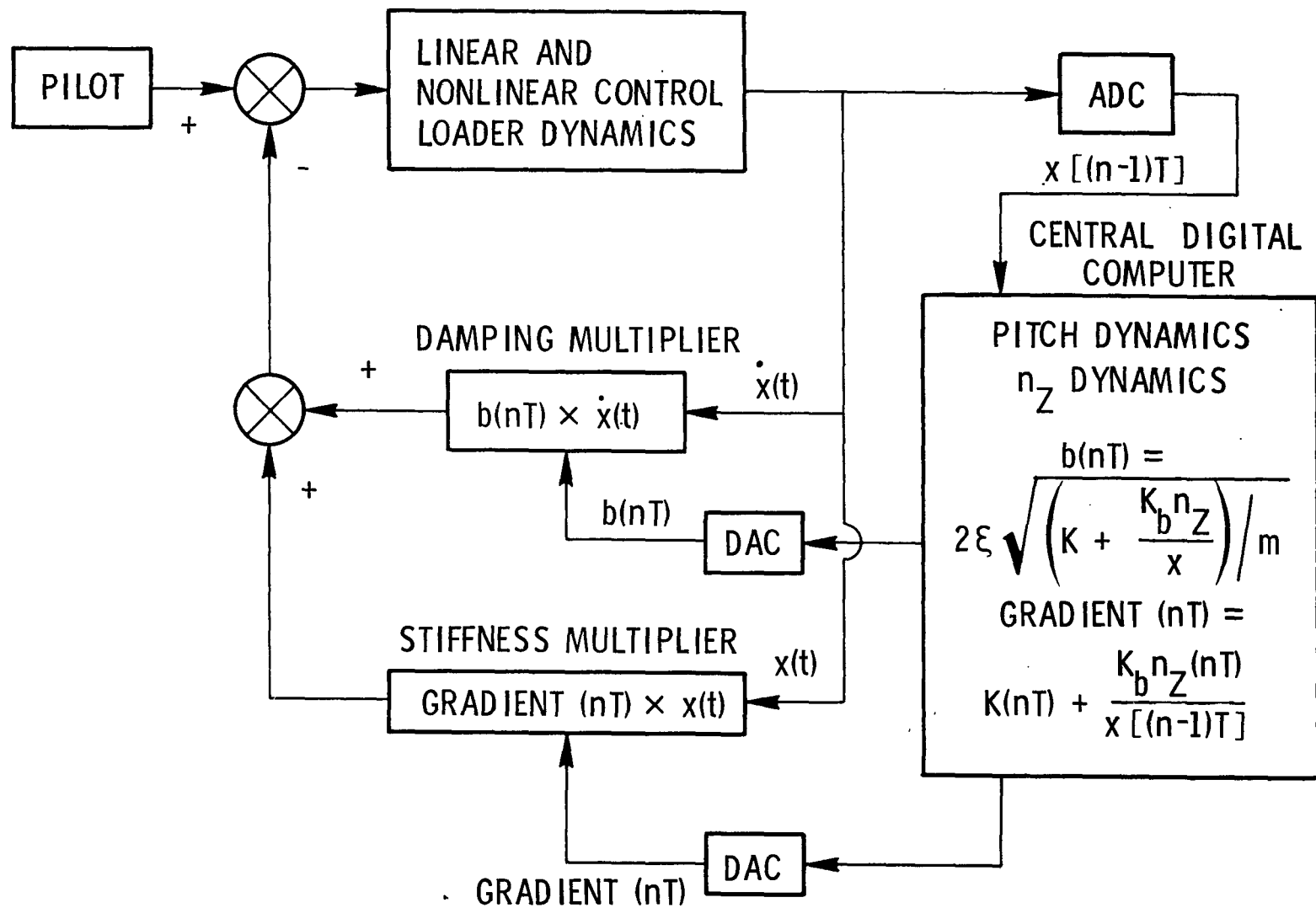


Figure 14.- Proposed control loader-central digital computer tie-in.



018 001 C1 U A 770107 S00903DS
DEPT OF THE AIR FORCE
AF WEAPONS LABORATORY
ATTN: TECHNICAL LIBRARY (SUL)
KIRTLAND AFB NM 87117

TMMASTER: If Undeliverable (Section 158
Postal Manual) Do Not Return

"The aeronautical and space activities of the United States shall be conducted so as to contribute . . . to the expansion of human knowledge of phenomena in the atmosphere and space. The Administration shall provide for the widest practicable and appropriate dissemination of information concerning its activities and the results thereof."

—NATIONAL AERONAUTICS AND SPACE ACT OF 1958

NASA SCIENTIFIC AND TECHNICAL PUBLICATIONS

TECHNICAL REPORTS: Scientific and technical information considered important, complete, and a lasting contribution to existing knowledge.

TECHNICAL NOTES: Information less broad in scope but nevertheless of importance as a contribution to existing knowledge.

TECHNICAL MEMORANDUMS: Information receiving limited distribution because of preliminary data, security classification, or other reasons. Also includes conference proceedings with either limited or unlimited distribution.

CONTRACTOR REPORTS: Scientific and technical information generated under a NASA contract or grant and considered an important contribution to existing knowledge.

TECHNICAL TRANSLATIONS: Information published in a foreign language considered to merit NASA distribution in English.

SPECIAL PUBLICATIONS: Information derived from or of value to NASA activities. Publications include final reports of major projects, monographs, data compilations, handbooks, sourcebooks, and special bibliographies.

TECHNOLOGY UTILIZATION PUBLICATIONS: Information on technology used by NASA that may be of particular interest in commercial and other non-aerospace applications. Publications include Tech Briefs, Technology Utilization Reports and Technology Surveys.

Details on the availability of these publications may be obtained from:

SCIENTIFIC AND TECHNICAL INFORMATION OFFICE

NATIONAL AERONAUTICS AND SPACE ADMINISTRATION

Washington, D.C. 20546